

# Synthesis $\text{Nd}_2\text{TiO}_5$ nanoparticles with different morphologies by novel approach and its photocatalyst application

Farhad Ahmadi<sup>1,2</sup> · Mehdi Rahimi-Nasrabadi<sup>3,4</sup> · Mohsen Behpour<sup>5</sup>

Received: 25 June 2016 / Accepted: 3 September 2016 / Published online: 7 September 2016  
© Springer Science+Business Media New York 2016

**Abstract** Nowadays, in connection with the increasing pollution of the environment, several studies are performed in order to find new group of compounds which could replace chemical synthesis capping agents due to their high toxicity to ecosystem and difficulty in being degraded in the environment. In the current study, an attempt is made to synthesize neodymium titanate ( $\text{Nd}_2\text{TiO}_5$ ) nanoparticles through a novel approach with the aid of capping agents such as alanine, leucine, and histidine in an aqueous solution and investigate their effect on the morphology and particle size of final products. According to the vibrating sample magnetometer result,  $\text{Nd}_2\text{TiO}_5$  nanoparticles indicated a paramagnetic behavior at room temperature. In addition, methyl orange was chosen as a dye water pollution to evaluate its degradation by  $\text{Nd}_2\text{TiO}_5$  nanoparticles under ultraviolet light irradiation. Furthermore, the photocatalysis results reveal that the maximum decolorization of 63 % for methyl orange occurred with  $\text{Nd}_2\text{TiO}_5$  nanoparticles in 60 min under ultraviolet light irradiation.

## 1 Introduction

Materials at the nanometer scale have been studied for decades because of their unique properties arising from the large fraction of atoms residing on the surface, and also from the finite number of atoms in each crystalline core. Especially, because of the increasing need for high area density storage, the synthesis and characterization nanocrystals have been extensively investigated [1–7]. Recently, extensive researches on the environmental problems, especially photocatalytic applications have been performed. The decolorization of hazardous organic dyes such as rhodamine B (RhB), methylen blue (MB), and methyl orange are very important, because their discharge from industrial applications causes severe adverse effects to the environment and greatly increases the water pollution and hence effectively disturbs the ecosystem [8–11]. Furthermore studies on thermophysical properties, including thermal expansion and heat capacity of  $\text{Ln}_2\text{TiO}_5$  (e.g.  $\text{Dy}_2\text{TiO}_5$ ,  $\text{Gd}_2\text{TiO}_5$ ,  $\text{Eu}_2\text{TiO}_5$ ), demonstrate their advantages of thermal stability with low swelling at high temperature (up to 1500 K), desired for control rod materials [12, 13]. In addition, the nanocluster form of yttrium titanate found its application in oxide-dispersion-strengthened steel when it was dispersed in ferritic alloy. This alloy is considered as the most promising structural material for advanced nuclear systems due to its greatly enhanced creep resistance at high temperature [14, 15] and exceptional radiation resistance originating from stabilized oxide nanoclusters. However, the structure and chemistry of the nanocluster oxides have not been fully understood, remaining one of the challenging scientific issues in nuclear materials research [16, 17]. In this report, for the first time, we had presented the preparation of  $\text{Nd}_2\text{TiO}_5$  nanoparticles by sol–gel method in the presence of alanine,

✉ Farhad Ahmadi  
Farhadahmadi55@gmail.com

✉ Mehdi Rahimi-Nasrabadi  
Rahiminasrabadi@gmail.com

<sup>1</sup> Physiology Research Center, School of Medicine, Iran University of Medical Sciences, Tehran, Iran

<sup>2</sup> Department of Medicinal Chemistry, School of Pharmacy-International Campus, Iran University of Medical Sciences, Tehran, Iran

<sup>3</sup> Department of Chemistry, Imam Hossein University, Tehran, Iran

<sup>4</sup> Faculty of Pharmacy, Baqiyatallah University of Medical Sciences, Tehran, Iran

<sup>5</sup> Institute of Nano Science and Nano Technology, University of Kashan, P. O. Box 87317-51167, Kashan, IR, Iran

leucine, and histidine without adding external surfactant. A simple approach for  $\text{Nd}_2\text{TiO}_5$  nanoparticles synthesis by utilizing natural template permits the reaction to proceed usually in milder conditions. Although existing chemical approaches have effectively produced well defined  $\text{Nd}_2\text{TiO}_5$  nanoparticles, these processes are generally costly and include the employ of toxic chemicals. The photocatalytic degradation was investigated using methyl orange (MO) under ultraviolet light irradiation [18–26].

## 2 Experimental

### 2.1 Characterization

X-ray diffraction (XRD) pattern was recorded by a Philips-X'PertPro, X-ray diffractometer using Ni-filtered  $\text{Cu K}\alpha$  radiation at scan range of  $10 < 2\theta < 80$ . Scanning electron microscopy (SEM) images were obtained on LEO-1455VP equipped with an energy dispersive X-ray spectroscopy. The electronic spectra were obtained on a Scinco UV–Vis scanning spectrometer (Model S-10 4100). The energy dispersive spectrometry (EDS) analysis was studied by XL30, Philips microscope. The magnetic measurement of sample was carried out in a vibrating sample magnetometer (VSM; Meghnatis Daghigh Kavir Co.; Kashan Kavir; Iran) at room temperature.

### 2.2 Synthesis of $\text{Nd}_2\text{TiO}_5$ nanoparticles

The amino acids, neodymium salt, ethanol, and tetra-*n*-butyl titanate (TNBT) were purchased from Merck Company and used without further purification. At first, a

**Table 1** The preparation conditions of the  $\text{Nd}_2\text{TiO}_5$  nanoparticles

Sample no.	Temperature	Capping agent	Degradation (%)
1	900	Alanine	63
2	900	Leucine	–
3	900	Histidine	–

stoichiometric amount of TNBT and neodymium nitrate (1:1) was separately dissolved in ethanol in two A and B beakers, respectively. Then, amino acid as capping agent was dissolved in ethanol and added to the A solution under constant stirring. Afterwards, the neodymium nitrate solution was mixed with solution under stirring at room temperature. Subsequently, the final mixed solution was kept stirring to form a gel at 90 °C. Finally, the obtained product was calcinated at different temperatures for 3 h in a conventional furnace in air atmosphere, and calcination at different temperatures was carried out (Table 1).

### 2.3 Photocatalytic experimental

The methyl orange (MO) photodegradation was examined as a model reaction to evaluate the photocatalytic activities of the  $\text{Nd}_2\text{TiO}_5$  nanoparticles under ultraviolet light irradiations. The photocatalytic degradation was performed with 150 mL solution of methyl orange (0.0005 g) containing 0.1 g of  $\text{Nd}_2\text{TiO}_5$ . This mixture was aerated for 30 min to reach adsorption equilibrium. Later, in order to perform photocatalytic tests, the mixture was placed inside the photoreactor in which the vessel was 15 cm away from the ultraviolet source of 400 W mercury lamps at room temperature. Aliquots of the mixture were taken at definite interval of times during the irradiation (60 min) and after

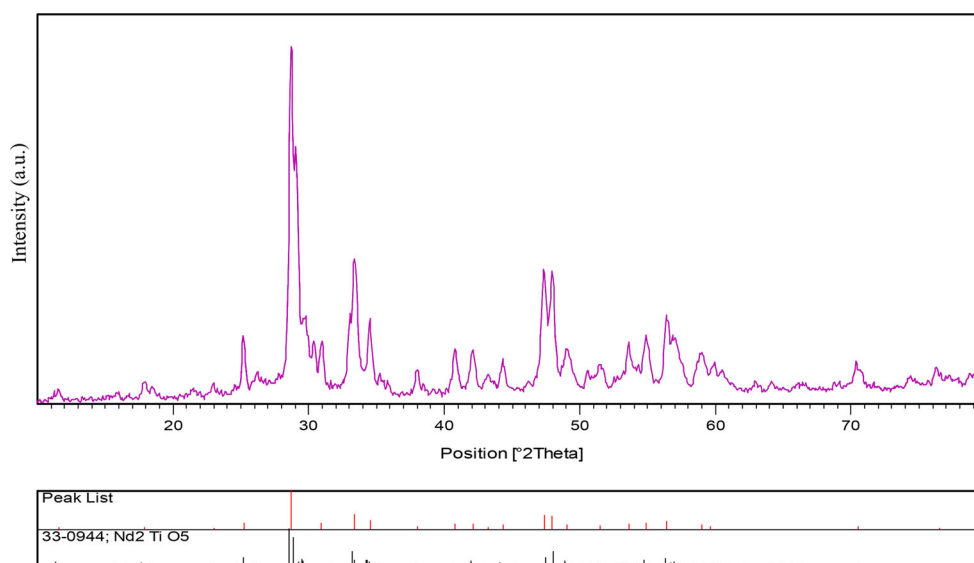


**Fig. 1** XRD pattern of  $\text{Nd}_2\text{TiO}_5$  nanoparticles calcined at 900 °C (sample 1)

centrifugation they were analyzed by a UV–Vis spectrometer. The methyl orange (MO) degradation percentage was calculated as:

$$\text{Degradation rate (\%)} = \frac{A_0 - A}{A_0} \times 100 \quad (1)$$

where  $A_0$  and  $A$  are the absorbance value of solution at  $A_0$  and  $A$  min, respectively.

### 3 Results and discussion

Crystalline structure and phase purity of as-prepared product has been determined using XRD. The XRD pattern of as-prepared  $\text{Nd}_2\text{TiO}_5$  (sample 1) is shown in Fig. 1. Based on the Fig. 1, the diffraction peaks observed can be indexed to pure orthorhombic phase of  $\text{Nd}_2\text{TiO}_5$

( $a = 10.7251 \text{ \AA}$ ,  $b = 11.3407 \text{ \AA}$ , and  $c = 3.8457 \text{ \AA}$ ) with space group of Pnam and JCPDS no. 33-0944. No diffraction peaks from other species could be detected, which indicates the obtained sample is pure. From XRD data, the crystallite diameter ( $D_c$ ) of  $\text{Nd}_2\text{TiO}_5$  nanoparticles (sample 1) was calculated to be 16 nm using the Scherer equation:  $D_c = K\lambda / \beta \cos\theta$  Scherer equation where  $\beta$  is the breadth of the observed diffraction line at its half intensity maximum,  $K$  is the so-called shape factor, which usually takes a value of about 0.9, and  $\lambda$  is the wavelength of X-ray source used in XRD. In the third millennium, current studies show that different type of capping agents such as ionic, polymeric; etc. play a fundamental role in synthesis procedures [27–38]. Moreover, capping agents are essential materials for preparation of many disperse systems such as solid/liquid dispersions (usually referred to as suspensions); therefore, in this research we examined the

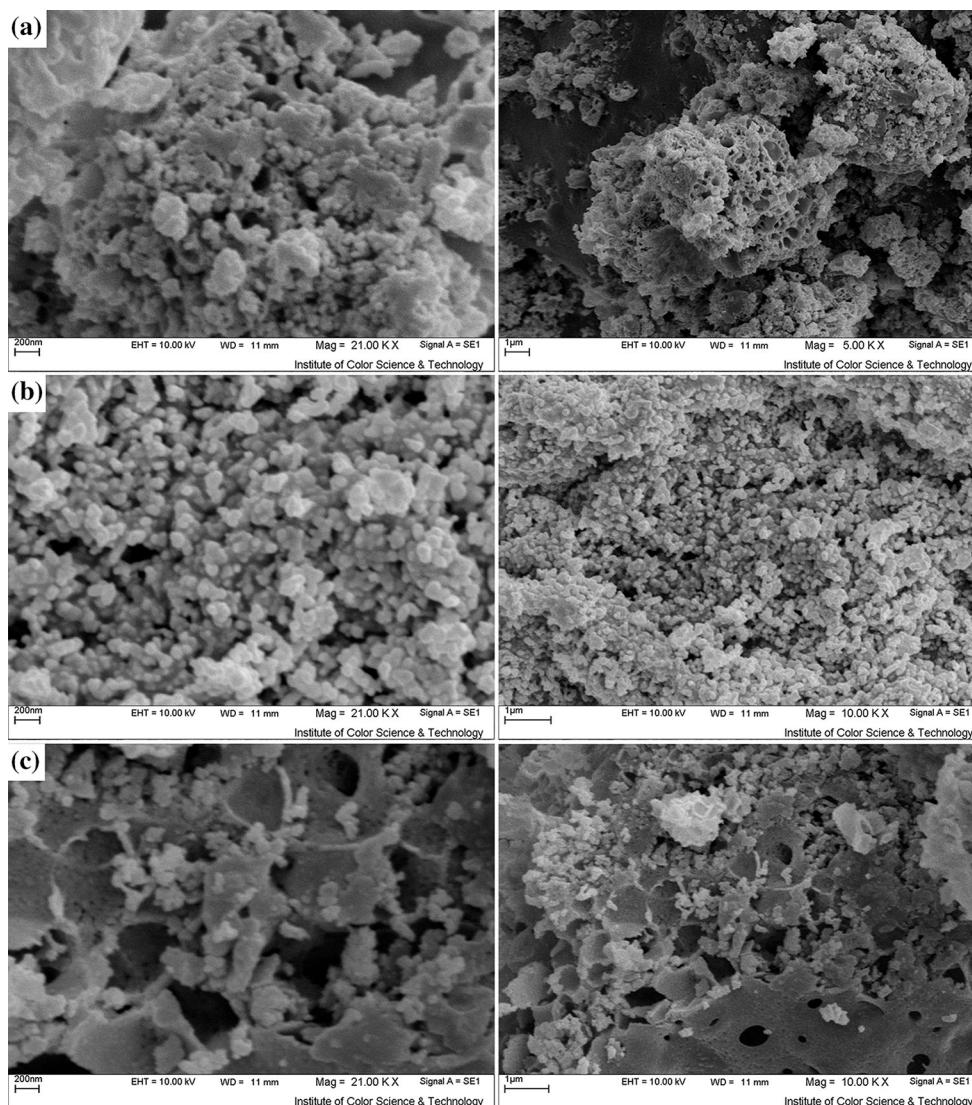


**Fig. 2** SEM images of  $\text{Nd}_2\text{TiO}_5$  nanoparticles calcined at 900 °C **a** sample 1, **b** sample 2 and **c** sample 3

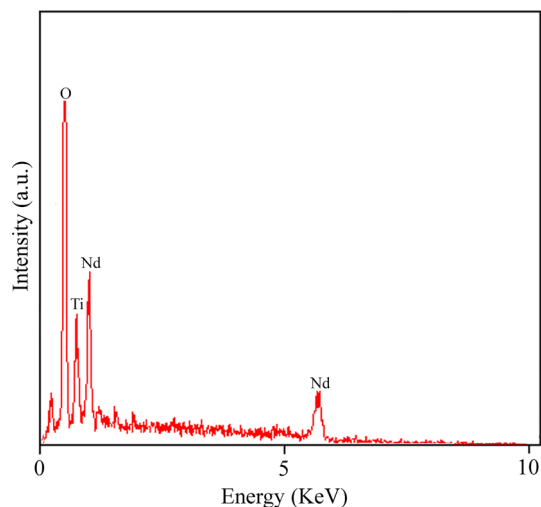
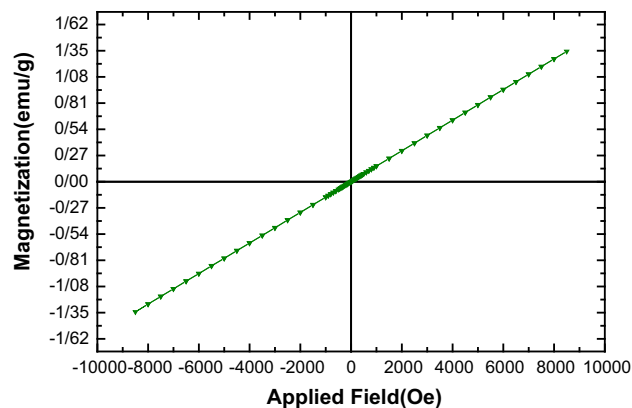


**Fig. 3** EDS pattern of  $\text{Nd}_2\text{TiO}_5$  nanoparticles calcined at  $900\text{ }^\circ\text{C}$  (sample 1)

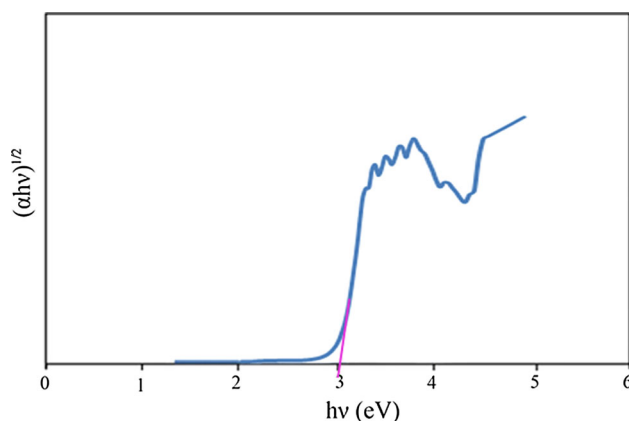
effect of capping agents such as alanine, leucine, and histidine on the morphology and particle size of final products. Figure 2a–c shows the SEM images of the sample 1–3, respectively. In the presence of capping agents (alanine and leucine), the product mainly consists of spherical shape nanoparticles with average particle size 40–45 nm, as shown in Fig. 2a, b. Besides, in the presence of histidine as the capping agents the particle size of products were increased and products become agglomerate, as shown in Fig. 2c. Therefore, amino acids cause to increase the particle size of final products. Therefore, amino acids cause to increase the particle size of final products. Since in this study we used amino acids; therefore, the EDS analysis measurement was used to investigate the chemical composition and purity of  $\text{Nd}_2\text{TiO}_5$  nanoparticles (sample 1), as shown in Fig. 3. According to the Fig. 3, the product consists of Ni, Ti, and O elements. Furthermore, neither N nor C signals were detected in the EDS spectrum, which means that the product is pure and free of any amino acids or impurity. The VSM magnetic measurement spectrum for the  $\text{Nd}_2\text{TiO}_5$  (Fig. 4) shows the magnetic properties of  $\text{Nd}_2\text{TiO}_5$  nanoparticles calcined at  $900\text{ }^\circ\text{C}$ . The  $\text{Nd}_2\text{TiO}_5$  nanoparticle (sample 1) exhibits ferromagnetic behavior at room temperature with a saturation magnetization of  $1.35\text{ emu/g}$ . The diffused reflectance spectrum of the as-prepared  $\text{Nd}_2\text{TiO}_5$  nanoparticles is shown in Fig. 5. The fundamental absorption edge in most semiconductors follows the exponential law. Using the absorption data the band gap was estimated by Tauc's relationship:

$$\alpha = \alpha_0(h\nu - E_g)^n/h\nu \quad (2)$$

where  $\alpha$  is absorption coefficient,  $h\nu$  is the photon energy,  $\alpha_0$  and  $h$  are the constants,  $E_g$  is the optical band gap of the material, and  $n$  depends on the type of electronic transition

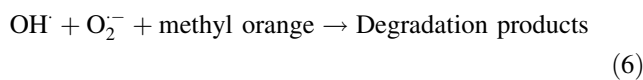
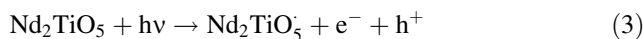


**Fig. 4** VSM curve of  $\text{Nd}_2\text{TiO}_5$  nanoparticles calcined at  $900\text{ }^\circ\text{C}$  (sample 1)



**Fig. 5** DRS pattern of  $\text{Nd}_2\text{TiO}_5$  nanoparticles calcined at  $900\text{ }^\circ\text{C}$  (sample 1)

and can be any value between  $\frac{1}{2}$  and 3. The energy gap of the  $\text{Nd}_2\text{TiO}_5$  nanoparticles (sample 1) is determined by extrapolating the linear portion of the plots of  $(\alpha h\nu)^{1/2}$  against  $h\nu$  to the energy axis, as shown in Fig. 5. The  $E_g$  value is calculated as  $3.0\text{ eV}$  for the  $\text{Nd}_2\text{TiO}_5$  nanoparticles. Photodegradation of methyl orange (MO) solution under UV light illumination was employed to evaluate the photocatalyst properties of the as-synthesized  $\text{Nd}_2\text{TiO}_5$  nanoparticles (Fig. 6). No methyl orange was practically broken down after 60 min in the absence of  $\text{Nd}_2\text{TiO}_5$  nanoparticles. The proposed mechanisms of the photocatalytic degradation of the methyl orange with the aid of  $\text{Nd}_2\text{TiO}_5$  nanoparticles can be assumed as:



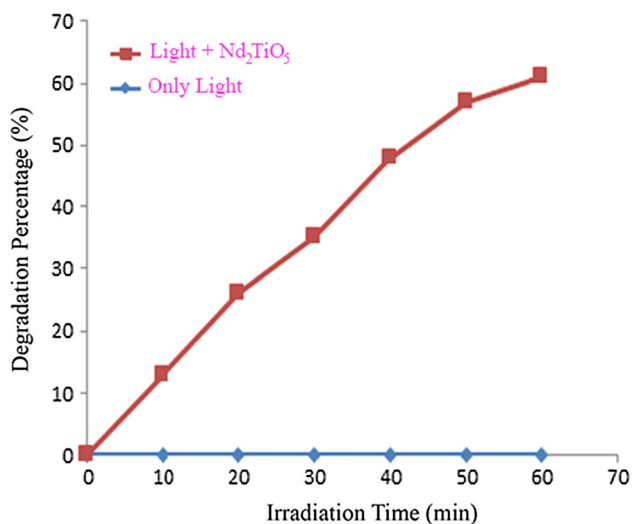
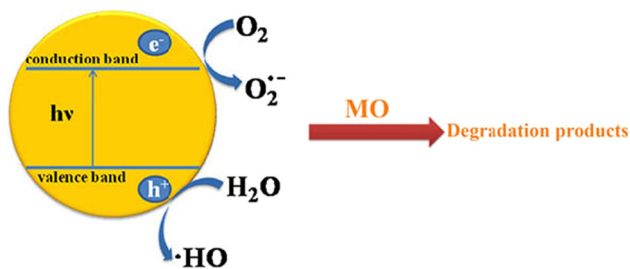


**Fig. 6** Photocatalytic methyl orange degradation of Nd<sub>2</sub>TiO<sub>5</sub> nanoparticles (sample 1) under ultraviolet light



**Scheme 1** Reaction mechanism of methyl orange photodegradation over Nd<sub>2</sub>TiO<sub>5</sub> nanoparticles under UV light irradiation

Utilizing photocatalytic calculations by Eq. (1), the methyl orange degradation was about 63 % after 60 min illumination of UV light in the presence of Nd<sub>2</sub>TiO<sub>5</sub> nanoparticles (sample 1). Besides, the whole mechanism is shown in Scheme 1.

## 4 Conclusions

In this work, Nd<sub>2</sub>TiO<sub>5</sub> nanoparticles were successfully synthesized by green method in an aqueous solution. EDS and XRD results proved high purity of the as-prepared Nd<sub>2</sub>TiO<sub>5</sub> nanoparticles. In order to investigate the effect of polymeric surfactants on the morphology and particle size of final products several tests were performed in the presence of alanine, leucine, and histidine. Applying nanocrystalline Nd<sub>2</sub>TiO<sub>5</sub> as the photocatalyst causes maximum 63 % degradation of methyl orange after 60 min irradiation of UV light. This result suggests that as-obtained nanocrystalline Nd<sub>2</sub>TiO<sub>5</sub> as favorable material has high potential to be used for photocatalytic applications under UV light.

**Acknowledgments** We gratefully acknowledge Vice Chancellor for Research and Technology, Iran University of Medical Sciences for financial support with Grant Number 26950.

## References

1. V. Arabali, M. Ebrahimi, M. Abbasghorbani, V.K. Gupta, M. Farsi, M.R. Ganjali, F. Karimi, *J. Mol. Liq.* **213**, 312 (2016)
2. H.R. Naderi, P. Norouzi, M.R. Ganjali, *Appl. Surf. Sci.* **366**, 552 (2016)
3. S.M. Hosseinpour-Mashkani, A. Sobhani-Nasab, *J. Mater. Sci. Mater. Electron.* **27**, 3240 (2016)
4. M. Zahraei, A. Monshi, D. Shahbazi-Gahrouei, M. Amirnasr, B. Behdadfar, M. Rostami, *J. Nanostruct.* **5**, 137 (2015)
5. M. Rahimi-Nasrabadi, *J. Nanostruct.* **4**, 211 (2014)
6. M. Maddahfar, M. Ramezani, M. Sadeghi, A. Sobhani-Nasab, *J. Mater. Sci.: Mater. Electron.* **26**, 7745 (2015)
7. S. Khaleghi, *J. Nanostruct.* **2**, 157 (2012)
8. M. Aliahmad, A. Rahdar, Y. Azizi, *J. Nanostruct.* **4**, 145 (2014)
9. M. Enhessari, M. Kargar-Razi, P. Moarefi, A. Parviz, *J. Nanostruct.* **2**, 119 (2012)
10. M. Behpour, M. Mehrzad, S.M. Hosseinpour-Mashkani, *J. Nanostruct.* **5**, 183 (2015)
11. M. Riazian, *J. Nanostruct.* **4**, 433 (2014)
12. K.V. Syamala, G. Panneerselvam, G.G.S. Subramanian, M.P. Antony, *Thermochim. Acta* **475**, 76 (2008)
13. G. Panneerselvam, R.V. Krishnan, M.P. Antony, K. Nagarajan, T. Vasudevan, P.V. Rao, *J. Nucl. Mater.* **327**, 220 (2004)
14. T. Hayashi, P.M. Sarosi, J.H. Schneibel, M.J. Mills, *Acta Mater.* **56**, 1407 (2008)
15. M.J. Alinger, G.R. Odette, D.T. Hoelzer, *Acta Mater.* **57**, 392 (2009)
16. G.R. Odette, M.J. Alinger, B.D. Wirth, *Annu. Rev. Mater. Res.* **38**, 471 (2008)
17. A. Hirata, T. Fujita, Y.R. Wen, J.H. Schneibel, C.T. Liu, M.W. Chen, *Nat. Mater.* **10**, 922 (2011)
18. M. Ramezani, S.M. Hosseinpour-Mashkani, A. Sobhani-Nasab, H.G. Estarki, *J. Mater. Sci. Mater. Electron.* **26**, 7588 (2015)
19. A. Sobhani-Nasab, M. Rangraz-Jeddy, A. Avanes, M. Salavati-Niasari, *J. Mater. Sci.: Mater. Electron.* **26**, 9552 (2015)
20. A. Sobhani-Nasab, M. Behpour, *J. Mater. Sci.: Mater. Electron.* **27**, 1191 (2016)
21. A. Sobhani-Nasab, S.M. Hosseinpour-Mashkani, M. Salavati-Niasari, S. Bagheri, *J. Clust. Sci.* **26**, 1305 (2015)
22. A. Sobhani-Nasab, S.M. Hosseinpour-Mashkani, M. Salavati-Niasari, H. Taqiri, S. Bagheri, K. Saberyan, *J. Mater. Sci.: Mater. Electron.* **26**, 5735 (2015)
23. K. Adib, M. Rahimi-Nasrabadi, Z. Rezvani, S.M. Pourmortazavi, F. Ahmadi, H.R. Naderi, *J. Mater. Sci.: Mater. Electron.* **27**, 4541 (2016)
24. M. Rahimi-Nasrabadi, M. Behpour, A. Sobhani-Nasab, S.M. Hosseinpour-Mashkani, *J. Mater. Sci.: Mater. Electron.* **26**, 9776 (2015)
25. S.M. Hosseinpour-Mashkani, M. Maddahfar, A. Sobhani-Nasab, *J. Mater. Sci.: Mater. Electron.* **27**, 474 (2016)
26. S.S. Hosseinpour-Mashkani, S.S. Hosseinpour-Mashkani, A. Sobhani-Nasab, *J. Mater. Sci.: Mater. Electron.* **27**, 4351 (2016)
27. K. Saberyan, N.S. Mazhari, M. Rahiminezhad-Soltani, M.A. Mohsen, *J. Nanostruct.* **4**, 185 (2014)
28. J. Safaei-Ghomi, S. Zahedi, M. Javid, M.A. Ghasemzadeh, *J. Nanostruct.* **5**, 153 (2015)
29. S.M. Pourmortazavi, M. Rahimi-Nasrabadi, A.A. Davoudi-Dehaghani, A. Javidan, M.M. Zahedi, S.S. Hajimirsadeghi, *Mater. Res. Bull.* **47**, 1045 (2012)

30. M. Rahimi-Nasrabadi, S.M. Pourmortazavi, A.A. Davoudi-Dehaghani, S.S. Hajimirsadeghi, M.M. Zahedi, *Cryst. Eng. Comm.* **15**, 4077 (2013)
31. M. Behpour, M. Chakeri, *J. Nanostruct.* **2**, 227 (2012)
32. S.M. Pourmortazavi, M. Taghdiri, V. Makari, M. Rahimi-Nasrabadi, *Spectrochim. Acta A Mol. Biomol. Spectrosc.* **136**, 1249 (2015)
33. M. Rahimi-Nasrabadi, S.M. Pourmortazavi, M.R. Ganjali, *Mater. Manuf. Process.* **30**, 34 (2015)
34. S.M. Pourmortazavi, M. Rahimi-Nasrabadi, S.S. Hajimirsadeghi, *J. Dispers. Sci. Technol.* **33**, 254 (2012)
35. S.M. Hosseinpour-Mashkani, M. Ramezani, A. Sobhani-Nasab, M. Esmaili-Zare, *J. Mater. Sci. Mater. Electron.* **26**, 6086 (2015)
36. A. Sobhani-Nasab, M. Maddahfar, S.M. Hosseinpour-Mashkani, *J. Mol. Liq.* **216**, 1 (2016)
37. S.M. Pourmortazavi, M. Rahimi-Nasrabadi, M. Khalilian-Shalamzari, H.R. Ghaeni, S.S. Hajimirsadeghi, *J. Inorg. Organomet. Polym. Mater.* **24**, 333 (2014)
38. M. Rahimi-Nasrabadi, S.M. Pourmortazavi, M.R. Ganjali, S.S. Hajimirsadeghi, M.M. Zahedi, *J. Mol. Struct.* **1047**, 31 (2013)